Characteristics of Five-Coordinate Nickel−Cysteine Centers

Patrick J. Desrochers,* Russell W. Cutts, Phillip K. Rice, and Melissa L. Golden

Department of Chemistry, University of Central Arkansas, Conway, Arkansas 72035

James B. Graham

Department of Chemistry, Henderson State University, Arkadelphia, Arkansas 71999

Tosha M. Barclay and A. W. Cordes

Department of Chemistry, University of Arkansas, Fayetteville, Arkansas 72701−1201

Received January 8, 1999

Monomeric five-coordinate nickel−cysteine complexes were prepared using anionic tris(3,5-disubstituted pyrazolyl)-borates (Tp^{*-} and Tp^{PhMe-}) and *l*-cysteine (ethyl ester and amino acid forms). Tp*NiCysEt crystallizes with a single methanol of solvation in the monoclinic space group $P2_1$: $a = 7.8145(18)$, $b = 24.201(6)$, $c = 7.9925(14)$ Å; $\beta = 117.991(16)°$. [Tp*NiCys$^-$][K$^+$] and Tp^{PhMe}NiCysEt show magnetic and electronic characteristics similar to Tp*NiCysEt, so that the trigonal bipyramidal coordination geometry confirmed for Tp*NiCysEt in the solid state likely applies to all three. All three complexes have high spin magnetic ground states at room temperature ($\mu_{eff} = 2.9-3.2\ \mu_B$, $S = 1$). Their electronic spectra are dominated by sulfur to nickel charge-transfer bands (388−430 nm in chloroform) with energies that correlate to respective thiolate basicities and Tp^{X-} donor strengths. The Tp* derivatives undergo a rapid reaction with molecular oxygen. Stoichiometric, infrared, and electronic spectroscopy measurements are consistent with formation of a sulfinate as a result of reaction with dioxygen. Kinetics measurements for the reaction of Tp*NiCysEt and O_2 fit the following composite rate law: rate $= k_1$[Tp*NiCysEt] $+ k_2[O_2]$[Tp*NiCysEt] with $k_1 = 0.013(1)$ min^{-1} and $k_2 = 4.8(1)$ M^{-1}·min^{-1} at 22 °C. Increased nucleophilicity of the nickel−sulfur center enhanced by electron donation from Tp^{*-} (vs Tp^{PhMe-}) and encouraged by a trigonal bipyramidal geometry (vs square planar $Ni(CysEt)_2$) is hypothesized as the reason for the susceptibility of Tp*NiCys complexes to oxygen.

Introduction

Extensive spectroscopic measurements[1] and a single-crystal X-ray diffraction study[2] have identified cysteine as the sulfur source binding nickel at the active sites of nickel-containing hydrogenase enzymes. These enzymes reversibly catalyze the reaction $H_2 \rightleftharpoons 2H^+ + 2e^-$,[3] and those from *D. gigas* and *T. Roseopersicina* bacteria are among the most widely studied to date. Many nickel−hydrogenase characteristics have been mimicked by synthetic models, including redox potentials,[4] EPR signals,[5] substrate binding,[6] hydrogen generation,[7] and oxidative deactivation.[4a,8−10]

(1) (a) Gu, Z.; Dong, J.; Allan, C. B.; Choudhury, S. B.; Franco, R.; Moura, J. J. G.; Moura, I.; LeGall, J.; Przybyla, A. E.; Roseboom, W.; Albracht, S. P. J.; Axley, M. J.; Scott, R. A.; Maroney, M. J. *J. Am. Chem. Soc.* **1996**, *118*, 11155. (b) Gessner, C.; Trofanchuk, O.; Kawagoe, K.; Higuchi, Y.; Yasuoka, N.; Lubitz, W. *Chem. Phys. Lett.* **1996**, *256*, 518. (c) van Elp, J.; Peng, G.; Zhou, Z. H.; Adams, M. W. W.; Baidya, N.; Mascharak, P. K.; Cramer, S. P. *Inorg. Chem.* **1995**, *34*, 2501. (d) Huang, Y.-H.; Park, J.-B.; Adams, M. W. W.; Johnson, M. K. *Inorg. Chem.* **1993**, *32*, 375. (e) Whitehead, J. P.; Gurbiel, R. J.; Bagyinka, C.; Hoffman, B. M.; Maroney, M. J. *J. Am. Chem. Soc.* **1993**, *115*, 5629. (f) Maroney, M. J.; Colpas, G. J.; Bagyinka, C.; Baidya, N.; Mascharak, P. K. *J. Am. Chem. Soc.* **1991**, *113*, 3962. (g) Colpas, G. J.; Maroney, M. J.; Bagyinka, C.; Kumar, M.; Willis, W. S.; Suib, S. L.; Baidya, N.; Mascharak, P. K. *Inorg. Chem.* **1991**, *30*, 920. (h) Whitehead, J. P.; Colpas, G. J.; Bagyinka, C.; Maroney, M. J. *J. Am. Chem. Soc.* **1991**, *113*, 6288. (i) Maroney, M. J.; Colpas, G. J.; Bagyinka, C. *J. Am. Chem. Soc.* **1990**, *112*, 7067.

(2) (a) Volbeda, A.; Charon, M.-H.; Piras, C.; Hatchiklan, E. C.; Frey, M.; Fontecilla-Camps, J. C. *Nature* **1995**, *373*, 580. (b) Volbeda, A.; Garcin, E.; Piras, C.; de Lacey, A. L.; Fernandez, V. M.; Hatchikian, E. C.; Frey, M.; Fontecilla-Camps, J. C. *J. Am. Chem. Soc.* **1996**, *118*, 12989.

(3) (a) Cammack, R. *Nature* **1995**, *373*, 556. (b) Roberts, L. M.; Lindahl, P. A. *Biochemistry* **1994**, *33*, 14339. (c) Hausinger, R. P. *Biochemistry of Nickel*; Plenum Press: New York, 1993. (d) Przybyla, A. E.; Robbins, J.; Menon, N.; Peck, H. D., Jr. *Microbiol. Rev.* **1992**, *88*, 109.

(4) (a) Buonomo, R. M.; Font, I.; Maguire, M. J.; Reibenspies, J. H.; Tuntulani, T.; Darensbourg, M. Y. *J. Am. Chem. Soc.* **1995**, *117*, 963. (b) Krüger, H.-J.; Peng, G.; Holm, R. H. *Inorg. Chem.* **1991**, *30*, 734. (c) Krüger, H.-J.; Holm, R. H. *J. Am. Chem. Soc.* **1990**, *112*, 2955.

(5) (a) Ge, P.; Riordan, C. G.; Yap, G. P. A.; Rheingold, A. L. *Inorg. Chem.* **1996**, *35*, 5408. (b) Baidya, N.; Olmstead, M. M.; Mascharak, P. K. *J. Am. Chem. Soc.* **1992**, *114*, 9666. (c) Sugiura, Y.; Kuwahara, J.; Suzuki, T. *Biochem. Biophys. Res. Commun.* **1983**, *115*, 878.

(6) (a) Liaw, W.-F.; Horng, Y.-C.; Ou, D.-S.; Ching, C.-Y.; Lee, G.-H.; Peng, S.-M. *J. Am. Chem. Soc.* **1997**, *119*, 9299. (b) Nguyen, D. H.; Hsu, H.-F.; Millar, M.; Koch, S.; Achim, C.; Bominaar, E. L.; Münck, E. *J. Am. Chem. Soc.* **1996**, *118*, 8963. (c) Marganian, C. A.; Vazir, H.; Baidya, N.; Olmstead, M. M.; Mascharak, P. K. *J. Am. Chem. Soc.* **1995**, *117*, 1584. (d) Baidya, N.; Olmstead, M.; Mascharak, P. K. *Inorg. Chem.* **1991**, *30*, 929.

(7) (a) Musie, G.; Reibenspies, J. H.; Darensbourg, M. Y. *Inorg. Chem.* **1998**, *37*, 302. (b) James, T. L.; Cal, L.; Muetterties, M. C.; Holm, R. H. *J. Am. Chem. Soc.* **1996**, *35*, 4148. (c) Bănică, F. G. *Bull. Soc. Chim. Fr.* **1991**, *128*, 697. (d) Bănică, F. G.; Diacu, E. *Collect. Czech. Chem. Commun.* **1991**, *56*, 140.

(8) Grapperhaus, C. A.; Darensbourg, M. Y *Acc. Chem. Res.* **1998**, *31*, 451.

10.1021/ic990059a CCC: $18.00
Published on Web 11/16/1999

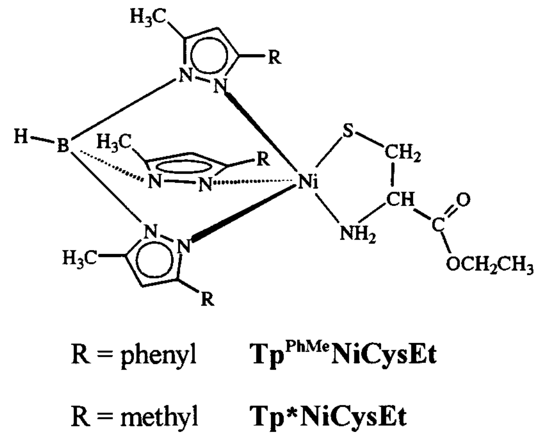

Figure 1. Coordination geometry of Tp^XNiCysEt complexes.

The nickel−cysteine geometries of these enzymes are unlike most synthetic nickel−cysteine complexes where square planar chelation predominates. Typical square planar complexes include $Ni(Cys)^{-2}$ and $Ni(CysEt)_2$[11] and peptide complexes such as $Ni(Cys\text{-}Gly)_2$ [12] and $Ni(Cys\text{-}Cys)_2$.[13] Novel nickel−cysteine geometries, unlike those previously seen in synthetic nickel−cysteine work, can add to the understanding of the interaction of this important bioligand with nickel.

The present work shows that facial tridentate ligands such as Tp^{PhMe-} and Tp^{*-} (Figure 1)[14] yield stable atypical nickel−cysteine coordination spheres. Tp*NiCysEt described here completes the series of Tp*MCysEt complexes (M = Co, Ni, Cu).[15] Its electronic characteristics fit neatly into this series, and its solid state molecular structure hints at likely structural characteristics of the more transient cobalt and copper homologues.

The trigonal bipyramidal geometry of Tp*NiCysEt introduces a pronounced oxygen sensitivity missing in the square planar $Ni(CysEt)_2$ complex. Nickel thiolate oxidation remains a model of oxidative deactivation of nickel−hydrogenases.[8,9] The present work supports this hypothesis, now directed at a nickel−cysteine center.

Experimental Section

Reagents and solvents were used as received from Aldrich Chemical Co. and Fisher. Elemental analyses were performed by Atlantic Micro Labs, Norcross, GA. Electronic spectra were recorded using a Perkin-Elmer Lambda 3 spectrometer and 1 cm quartz cells. Infrared spectra were recorded using a Nicolet Magna-IR 560 FT spectrometer and KBr pellets. Magnetic susceptibilities were measured for packed solid samples in a Johnson Matthey MSB-1 susceptibility balance. All measurements were recorded at ambient temperature.

Syntheses. The syntheses of the new ligand, Tp^{PhMe-}, two nickel thiolate precursors, Tp^{PhMe}NiCl and Tp^*NiNO_3,[16] and details of the chromatographic purification of Tp^{PhMe}NiCysEt and $[Tp^*NiCys^-][K^+]$ are described in Supporting Information. Table 1 summarizes characteristics of the Tp^XNiCys complexes.

Tp^{PhMe}NiCysEt. A solution of *l*-cysteine ethyl ester hydrochloride (0.096 g, 0.52 mmol) and triethylamine (0.15 mL, 1.1 mmol) in 120 mL of chloroform was added to a 15 mL chloroform solution of Tp^{PhMe}-NiCl (0.31 g, 0.52 mmol). The lime green color of the adduct developed immediately; this mixture was stirred for an additional 15 min. Chromatographic purification gave the lime green solid (yield: 0.25 g, 66%).

Tp*NiCysEt. A solution of *l*-cysteine ethyl ester hydrochloride (0.063 g, 0.34 mmol) and triethylamine (0.10 mL, 0.72 mmol) was prepared under nitrogen in 3 mL of degassed methanol. This solution was added via cannula to a light blue solution of Tp^*NiNO_3 (0.152 g, 0.36 mmol, in 30 mL of methanol). An emerald green solution developed immediately, and the product precipitated within 5 min. The mixture was stirred for an additional 20 min while immersed in an ice bath. The green solid was filtered under nitrogen, washed with 5 mL portions of cold methanol, and dried in vacuo under nitrogen (yield: 0.10 g, 55%). The reaction filtrate at −5 °C produced green X-ray quality crystals after 4 days.

$[Tp^*NiCys^-][K^+]$. Tp^*NiNO_3 (300 mg, 0.72 mmol) was dissolved in a minimum of degassed methanol. To this solution was added via cannula 8.8 mL of a methanolic cysteine solution (100 mg of KOH; 96 mg of *l*-cysteine, 0.79 mmol; 10 mL of methanol). Cysteine addition produced a clear deep green solution. Following 5 min additional stirring, this was stripped to dryness. Purification by column chromatography under nitrogen gave the green solid product (yield: 0.15 g, 41%).

Kinetics Measurements. Reaction mixtures were prepared in a 100 mL flask under nitrogen. A representative run used 34 mg of Tp*NiCysEt, 1.2 g of tetrabutylammonium tetrafluoroborate ($I = 0.073$ M, greater than 50-fold molar excess), and 50 mL of methanol. Variable nitrogen/oxygen gas mixtures were prepared using calibrated flowmeters and a gas mixing chamber. Constant dissolved oxygen concentrations were ensured by continuous sparging of the reaction solution with the gas mixture at a fixed oxygen partial pressure. Reaction aliquots were removed via a syringe and septum fitting on the reaction flask, and decreasing absorbance at 400 nm (A_{400}) measurements were taken every 3−5 min in a septum-fitted quartz cuvette.

Crystallography. Data were collected using the $\theta-2\theta$ technique and an ENRAF-Nonius CAD-4 diffractometer for a crystal of $Tp^*NiCysEt{\cdot}CH_3OH$ embedded in epoxy, sealed into a glass capillary. Table 2 summarizes the crystallographic parameters. The structure was solved by direct methods using NRCVAX software[17] and refined by full-matrix least-squares analysis. Non-hydrogen atoms were refined anisotropically, except for the two carbon atoms of the positionally disordered ethyl group of the ester. This group was refined isotropically and was best fit with 50/50 occupancy of two disordered positions. Hydrogen atoms were refined isotropically at idealized positions.

Results and Discussion

Anionic $^-$CysEt reacts with Tp^{PhMe}NiCl or Tp^*NiNO_3 to yield five-coordinate thermally stable adducts, Tp^XNiCysEt. Thiolate sulfur encourages this metathesis, because alanine, acid or ethyl ester, fails to displace nitrate from Tp^*NiNO_3 (by UV/vis, in the presence of triethylamine), and protonated cysteine ethyl ester is unreactive toward Tp^*NiNO_3 until triethylamine is added.

Tp*NiCysEt is more stable than the thermally sensitive cobalt and copper homologues.[15] Cobalt(II)'s propensity for tetrahedral geometries,[18] encouraged by the facial Tp^{*-} chelate, may drive the instability of Tp*CoCysEt. Tp*CuCysEt reportedly forms

(9) Maroney, M. J.; Choudhury, S. B.; Bryngelson, P. A.; Mirza, S.; Sherrod, M. J. *Inorg. Chem.* **1996**, *35*, 1073.
(10) (a) Choudhury, S. B.; Pressler, M. A.; Mirza, S. A.; Day, R. O.; Maroney, M. J. *Inorg. Chem.* **1994**, *33*, 4831. (b) Farmer, P. J.; Verpeaux, J.; Amatore, C.; Darensbourg, M. Y.; Musie, G. *J. Am. Chem. Soc.* **1994**, *116*, 9355. (c) Farmer, P. J.; Solouki, T.; Mills, D. K.; Soma, T.; Russell, D. H.; Reibenspies, J. H.; Darensbourg, M. Y. *J. Am. Chem. Soc.* **1992**, *114*, 4601. (d) Kumar, M.; Colpas, G. J.; Day, R. O.; Maroney, M. J. *J. Am. Chem. Soc.* **1989**, *111*, 8323.
(11) Baidya, N.; Ndreu, D.; Olmstead, M. M.; Mascharak, P. K. *Inorg. Chem.* **1991**, *30*, 2448.
(12) Kozlowski, H.; Decock-Le Révérend, B.; Ficheux, D.; Loucheux, C.; Sovago, I. *J. Inorg. Biochem.* **1987**, *29*, 187.
(13) Panossian, R.; Asso, M.; Guiliano, M. *Spectrosc. Lett.* **1983**, *16*, 463.
(14) Trofimenko, S. *Chem. Rev.* **1993**, *93*, 943.
(15) (a) Thompson, J. S.; Sorrell, T.; Marks, T. J.; Ibers, J. A. *J. Am. Chem. Soc.* **1979**, *101*, 4193. (b) Thompson, J. S.; Marks, T. J.; Ibers, J. A. *J. Am. Chem. Soc.* **1979**, *101*, 4180.
(16) Han, R.; Looney, A.; McNeil, K.; Parkin, G.; Rheingold, A. L.; Haggerty, B. S. *J. Inorg. Biochem.* **1993**, *49*, 105.
(17) Gabe, E. J.; Le Page, Y.; Charland, J.-P.; Lee, F. L.; White, P. S. *J. Appl. Crystallogr.* **1989**, *22*, 384−387.

Table 1. Physical and Analytical Data for Tp^XNi Complexes

complex	color	yield, %	anal.,[b] % C	H	N	ν(B−H),[c] cm^{-1}	μ_{eff}, μ_B	UV/vis,[d] nm (ϵ, $M^{-1}\cdot cm^{-1}$)
$Tp^{PhMe}NiCl$[a] ($C_{30}H_{28}BClN_6Ni$)	rose	76	59.01 (59.00)	4.69 (4.63)	13.61 (13.62)	2544		482 (280), 808 (65), 875 (60)
$Tp^{PhMe}NiCysEt$ ($C_{35}H_{38}BN_7NiO_2S$)	lime green	66	62.14 (60.90)	5.65 (5.55)	14.01 (14.20)	2550	2.91	433 (950), 634 (20)
Tp*NiCysEt ($C_{20}H_{32}BN_7NiO_2S$)	green	55	47.39 (47.65)	6.32 (6.41)	20.03 (19.46)	2518	3.11	388 (2670), 640 (87)
[Tp*NiCys$^-$][K^+] ($C_{18}H_{27}BKN_7NiO_2S$)	green	41	40.51 (42.05)	5.17 (5.26)	18.28 (19.08)	2513	3.22	397 (1770), 640 (72)

[a] Analyzed for $Tp^{PhMe}NiCl\cdot{}^1/_3CHCl_3$. [b] Calculated values in parentheses. [c] For KTp^{PhMe}, 2478 cm^{-1}; for KTp*, 2444 cm^{-1}. [d] $CHCl_3$ solutions.

Table 2. Crystal, Collection, and Refinement Parameters for Tp*NiCysEt·CH_3OH

formula	$NiC_{21}H_{36}BN_7O_3S$	max 2θ, deg	54
fw	536.2	std *h,k,l* indices	4, 9, −3; 2, 3, −5; 1, 4, 4
crystal size, mm	0.15 × 0.20 × 0.20	drift of stds, %	2.03
a, Å	7.8145(18)	absorption range	0.94−1.00
b, Å	24.201(6)	unique refls	2982
c, Å	7.9925(14)	*R* for merge	0.045
β, deg	117.991(16)	refls refined with $I > 1.0\sigma(I)$	2410
V, $Å^3$	1334.7(5)	parameters refined	304
2θ for cell, deg	26−28	R, R_w; for $I > 1.0\sigma(I)$	0.064, 0.067
d(calcd), g cm^{-3}	1.334	R, R_w; for $I > 3.0\sigma(I)$	0.046, 0.057
space group	$P2_1$	GOF	1.06
Z	2	p, $w^{-1} = [\sigma^2(I) + pI^2]/4F^2$	0.04
λ(Mo Kα_1), Å	0.7107	largest Δ/σ	0.005
h, *k*, *l* ranges	$0 \le h \le 10$; $-30 \le k \le +30$; $-10 \le l \le +10$	final diff map, e $Å^{-3}$	−0.67(5), +0.48(5)

green Tp*$CuSO_2$CysEt upon exposure to oxygen and warming to room temperature.[15b] Five-coordinate geometries are more common for nickel, and Tp*NiCysEt is stable for weeks at room temperature under nitrogen.

Crystal and Molecular Structure of Tp*NiCysEt. Tp*NiCysEt has a trigonal bipyramidal geometry in the solid state (Figure 2). The equatorial plane contains two Tp* nitrogen atoms and the sulfur, with the nickel atom only 0.063(6) Å from this plane. Distortions of in-plane angles from idealized values reflect the Tp*$^-$ bite angle, accommodation of the sulfur atom, and optimized overlap of the N2, N6, and S lone pairs mediated by the nickel d_{xy} orbital (vide infra). The third Tp* nitrogen and CysEt nitrogen occupy the axial positions.

Bond distances in Tp*NiCysEt are typical of Ni−Cys and Ni−Tp^X complexes. The equatorial nickel−nitrogen (Tp*) distances, 2.017(6) and 2.025(7) Å, compare to an average nickel−nitrogen (Tp^X) distance of 2.06(4) Å, calculated from three different (Tp^X)−nickel complexes.[19] A weaker axial ligand field is indicated by the longer axial nickel−nitrogen distances (Ni−N4, 2.125(7) Å and Ni−N1 2.175(7) Å). Nickel−nitrogen, 1.92(1) Å, and nickel−sulfur distances, 2.204(3) Å, in $K_2[Ni(Cys)_2]$[11] are both shorter than in Tp*NiCysEt, although the nickel−sulfur distance, 2.269(3) Å, in Tp*NiCysEt is typical of five-coordinate nickel thiolates.[6c,d,20] Cysteine ethyl ester chelate backbone distances in Tp*NiCysEt also agree with $K_2[Ni(Cys)_2]$. Weaker cysteine ethyl ester coordination is indicated for Tp*NiCysEt overall, distinguishing it from the square planar $[Ni(Cys)_2]^{2-}$ complex, where metal−ligand bonds are expected to be stronger.

(18) Cotton, F. A.; Wilkinson, G. *Advanced Inorganic Chemistry*, 5th ed.; Wiley-Interscience: New York, 1988; p 727.

(19) (a) Trofimenko, S.; Calabrese, J. C.; Kochi, J. K.; Wolowiec, S.; Hulsbergen, F. B.; Reedijk, J. *Inorg. Chem.* **1992**, *31*, 3943. (b) Bandoli, G.; Clemente, D. A.; Paolucci, G.; Doretti, L. *Cryst. Struct. Commun.* **1979**, *8*, 965.

(20) Shoner, S. C.; Olmstead, M. M.; Kovacs, J. A. *Inorg. Chem.* **1994**, *33*, 7.

Electronic Characteristics. Electronic spectra of Tp^XNi−SR complexes are qualitatively similar, dominated by an intense sulfur-to-nickel charge-transfer band (S→Ni CT), Figure 3. The S(Cys)→Ni CT energies of Tp^XNiCysEt are higher than the S(Cys)→Ni CT of nickel substituted azurins[21] and rubredoxins[22] with "D_{2d}" geometries and lower than the S(Cys)→Ni CT from square planar $Ni(Cys\text{-}Gly)_2$.[12] Tp^XNi−SR CT energies decrease with increasing Brønsted basicity of the sulfur donor.[23] MOPAC calculations[24] predict this trend of increasing sulfur lone pair energies with increasing sulfur basicity, a trend also supported by nickel selenates.[6d,10a,25]

Figure 4 summarizes electronic characteristics for the Tp^X-NiCys complexes. It describes a stronger equatorial ligand field. The S→Ni CT of Tp*NiCysEt (25 770 cm^{-1}) is between Tp*CoCysEt (29 410 cm^{-1})[15a] and Tp*CuCysEt (14 710 cm^{-1}),[15b,26] mirroring relative d-orbital energies. The S→Ni CT in Tp*Ni−SR complexes are blue shifted from Tp^{PhMe}Ni−SR analogues,[23] and $Fe(Tp^*)_2$ has a less positive iron(III/II) reduction potential than $Fe(Tp^{PhPh})_2$.[27] Therefore, the higher energy S→Ni CT of Tp*NiCysEt versus Tp^{PhMe}NiCysEt is consistent with a higher energy HOMO for the Tp*$^-$ complex.

Reaction of Tp*NiCysEt with O_2. Tp*NiCysEt and Tp*NiCys$^-$ both have a pronounced sensitivity to oxygen,

(21) Ferris, N. S.; Woodruff, W. H.; Tennent, D. L.; McMillin, D. R. *Biochem. Biophys. Res. Commun.* **1979**, *88*, 288.

(22) (a) Huang, Y.-H.; Moura, I.; Moura, J. J. G.; LeGall, J.; Park, J.-B.; Adams, M. W. W.; Johnson, M. K. *Inorg. Chem.* **1993**, *32*, 406. (b) Mus-Veteau, I.; Diaz, D.; Gracia-Mora, J.; Guigliarelli, G. C.; Bruschi, M. *Biochim. Biophys. Acta* **1991**, *1060*, 159.

(23) Supporting Information, Table S1.

(24) Stewart, J. J. P. *MOPAC*, Version 6.0; Serena Software: Bloomington, IN, 47402.

(25) Baidya, N.; Noll, B. C.; Olmstead, M. M.; Mascharak, P. K. *Inorg. Chem.* **1992**, *31*, 2999.

(26) Kitajima, N.; Fujisawa, K.; Tanaka, M.; Moro-oka, Y. *J. Am. Chem. Soc.* **1992**, *114*, 9232.

(27) (a) Gorrell, I. B.; Parkin, G. *Inorg. Chem.* **1990**, *29*, 2452. (b) Eichhorn, D. M.; Armstrong, W. H. *Inorg. Chem.* **1990**, *29*, 3607.

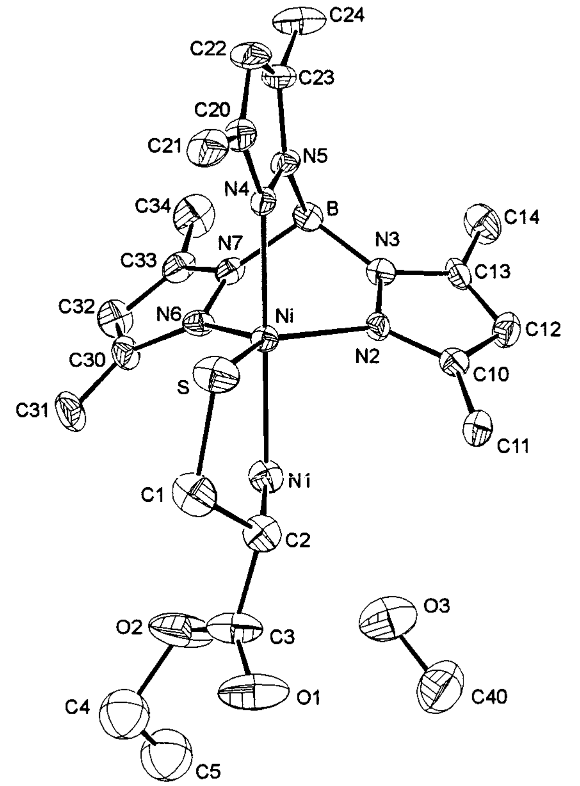

Figure 2. ORTEP drawing of Tp*NiCysEt·CH_3OH. 30% probabability ellipsoids are shown with hydrogen atoms omitted for clarity. Selected bond distances (Å) and angles (deg): Ni−S, 2.269(3); Ni−N1, 2.175(7); Ni−N2, 2.017(6); Ni−N4, 2.125(7); Ni−N6, 2.025(7); S−C1, 1.819(11); C1−C2, 1.522(14); C2−C3, 1.515(15); C3−O1, 1.189(15); C3−O2, 1.338(16); S−Ni−N1, 84.5(2); S−Ni−N2, 135.8(2); S−Ni−N4, 99.3(2); S−Ni−N6, 130.7(2); N1−Ni−N2, 91.3(3); N1−Ni−N4, 176.0(3); N1−Ni−N6, 90.6(3); N4−Ni−N6, 86.1(3); N2−Ni−N4, 86.8(3); N2−Ni−N6, 93.1(3); S−C1−C2, 111.8(7); N1−C2−C1, 109.5(8); C1−C2−C3, 108.8(9); C2−C3−O1, 122.7(11); O1−C3−O2, 124.7(11); O2−C4−C5, 102(3).

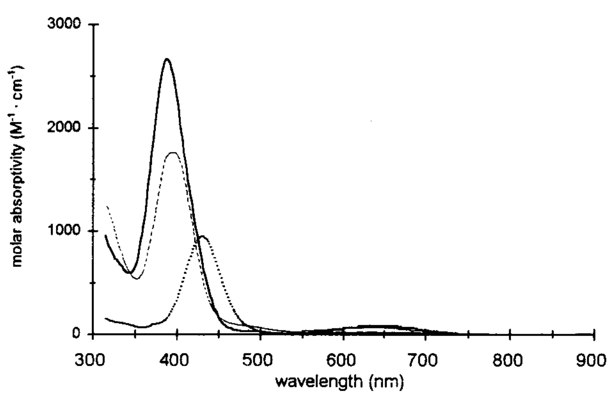

Figure 3. Electronic spectra of Tp*NiCysEt (—), [Tp*NiCys⁻][K⁺] (- - -), and Tp^{PhMe}NiCysEt (···) in chloroform.

similar to behavior reported for Tp*CuCysEt.[15b] Measurements for Tp*NiCysEt show it reacting with 1 equiv of dioxygen in methanol. The reaction of either Tp*NiCysEt or Tp*NiCys⁻ is characterized by loss of the S→Ni CT band, appearance of IR peaks in the 1100−1200 cm^{-1} region, suggestive of ν(S=O),[8,28] and no change in the pivotal ν(B−H) band. Readdition of unoxidized thiolate to these solutions returns the characteristic S→Ni CT bands. Breakage of the nickel−sulfur bond during

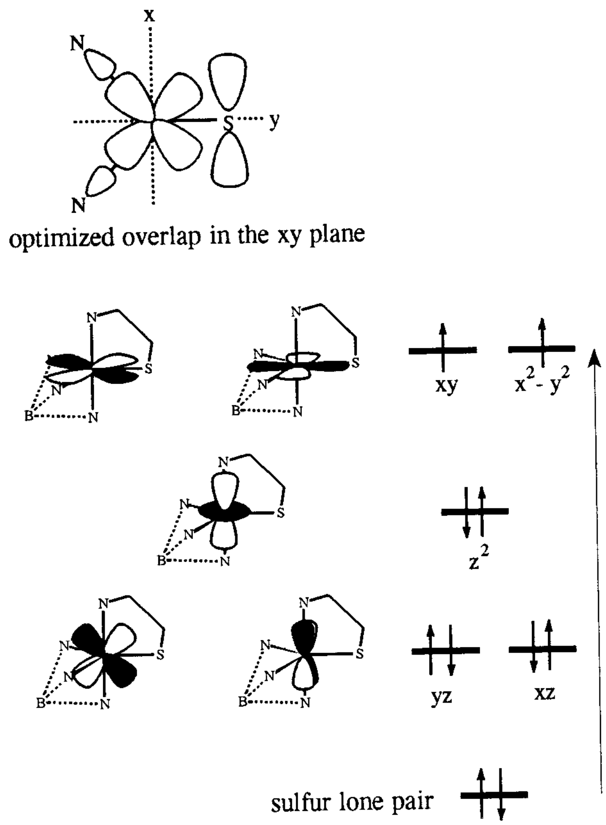

Figure 4. Proposed d orbital splitting diagram for Tp^XNiCysEt complexes. The vertical arrow represents the S→Ni CT. The top figure demonstrates optimized N−Ni−S overlap in the *xy* plane.

oxidation of Tp*NiCysEt is indicated by the loss of the S→Ni CT[29] as opposed to a shift in this band.[9] Cysteine ethyl ester thiolate (H−SR, pK_a = 6.5) conversion to a sulfinate (H−SO_2R, pK_a < 2) would reduce the sulfur basicity,[30] encouraging nickel−sulfur bond cleavage. Poorer sulfinate nucleophilicity is further supported by our observation that deprotonated cysteine sulfinate (Aldrich/Sigma) fails to displace nitrate from Tp*$NiNO_3$ in methanol. Despite nickel−sulfur bond cleavage in Tp*NiCysEt, oxidized CysEt⁻ remains bound to nickel. The insoluble thermodynamic product,[31] $(Tp^*)_2$Ni, was not observed, although anticipated from a coordinatively unsaturated Tp*Ni⁺ fragment that would result from complete CysEt⁻ displacement. Pale green oxidized Tp*NiCys complexes are unlike rose-colored four-coordinate Tp^XNi−Y complexes.[19a,27a,32] Oxidized Tp*NiCys complexes likely have five- or six-coordinate nickel geometries, with oxidized cysteine fragments chelating through sulfur−oxygen and unperturbed amine donors. More extensive characterization of these oxidized products is ongoing.

(28) Tyler, L. A.; Noveron, J. C.; Olmstead, M. M.; Mascharak, P. K. *Inorg. Chem.* **1999**, *38*, 616.

(29) Xu, Y.; Wilcox, D. E. *J. Am. Chem. Soc.* **1998**, *120*, 7375.

(30) pK_a < 2 for the sulfinate functionality of oxidized ⁻CysEt is based on a comparison with values for the amino acid itself. A pK_a of 8.3 is reported for the thiol group of cysteine. With oxidation, a much lower pK_a of 1.8 is reported for the H−SO_2R group of cysteine sulfinic acid. Because a lower pK_a of 6.5 is reported for the thiol of cysteine ethyl ester, it is reasonable to assume a correspondingly lower pK_a (less than 2) for the H−SO_2R group of the ethyl ester. pK_a values were taken from: *CRC Handbook of Biochemistry, Selected Data for Molecular Biology;* Sober, H. A., Ed.; CRC Press: Cleveland, OH, 1970; pp 200−23.

(31) Trofimenko, S. *J. Am. Chem. Soc.* **1967**, *89*, 6288.

(32) (a) Calabrese, J. C.; Trofimenko, S. *Inorg. Chem.* **1992**, *31*, 4810. (b) Trofimenko, S.; Calabrese, J. C.; Domaille, P. J.; Thompson, J. S. *Inorg. Chem.* **1989**, *28*, 1091. (c) Trofimenko, S.; Calabrese, J. C.; Thompson, J. S. *Inorg. Chem.* **1987**, *26*, 1507.

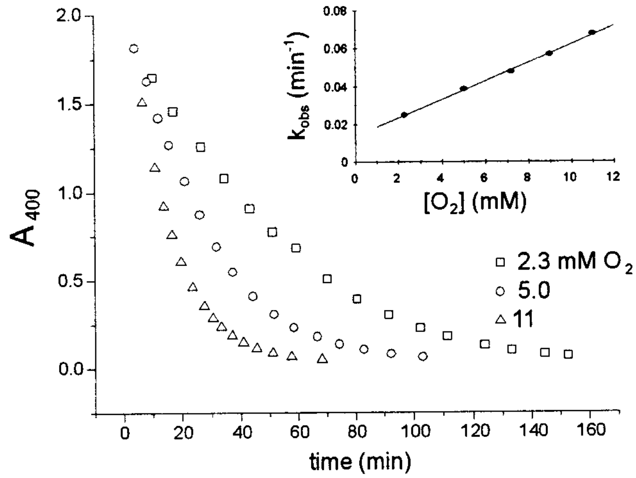

Figure 5. Dependence of A_{400} on dissolved oxygen concentration in the reaction between Tp*NiCysEt and O_2 in methanol. Dissolved oxygen concentrations were calculated using a Henry's Law constant of 1.42×10^{-5} M·Torr^{-1}, *Int. Crit. Tables* **1928**, *3*, 262. The data fit the rate law: $-d[\text{Tp*NiCysEt}]/dt = k_1[\text{Tp*NiCysEt}] + k_2[\text{Tp*NiCysEt}][O_2]$. The inset shows the linear dependence of k_{obs} on dissolved oxygen concentration. k_{obs} is the pseudo-first-order rate constant and is equal to $k_1 + k_2[O_2]$. Slope $= k_2 = 4.8(1)$ M^{-1} min^{-1} and intercept $= k_1 = 0.013(1)$ min^{-1}.

Kinetics of Tp*NiCysEt + O_2. Kinetics measurements for the Tp*NiCysEt + O_2 reaction monitored the diminishing S→Ni CT band (Figure 5). These data were best fit by a composite rate law with two competing rate-limiting steps.[33] One step may involve rate-limiting nickel−sulfur bond cleavage ($k_1 = 0.013(1)$ min^{-1}), followed by rapid O_2 attack at the free thiolate. A competing step may involve the concerted reaction of the nickel−sulfur center with the O_2 electrophile ($k_2 = 4.8(1)$ M^{-1}·min^{-1}) prior to nickel−sulfur bond rupture. Our $[O_2]$-dependent step dominates the rate law and is 4 times larger than that of Maroney's $[Ni(L)CN]^-$ complexes (L is a meridial, tridentate S,N-donor).[34] A competing first-order step was not reported nor expected for oxidation of square planar $[Ni(L)CN]^-$, because this would require three-coordinate nickel intermediates. The nickel−sulfur group of Tp*NiCysEt is more sterically encumbered than square planar $[Ni(L)CN]^-$; therefore this does not explain the marked difference in reaction rate. Although no kinetics measurements have been reported, square planar $Ni(CysEt)_2$ is considerably less oxygen sensitive than Tp*NiCysEt by our observations.

We hypothesize that electronic influence from the trigonal bipyramidal geometry encourages the greater oxygen sensitivity of Tp*NiCysEt. Electron donation from the two equatorial Tp* nitrogen atoms (N2 and N6) enhances the nucleophilicity of the nickel−sulfur bond. Figures 2 and 4 show that the N2− and N6−Ni−S bond angles (135.8° and 130.7°) optimize overlap of Tp* nitrogen lone pairs, the nickel d_{xy} orbital, and the in-plane sulfur p orbital. The O_2 electrophile could skirt the Tp*−methyl group and approach the nickel−sulfur group in the electron-rich equatorial plane. Diminished oxygen sensitivity of Tp^{PhMe}NiCysEt follows from diminished Tp^{PhMe} nitrogen electron donation, and a less electron-rich nickel−sulfur center. Experiments to test this hypothesis are ongoing.

Acknowledgment. Tom Heinze of the National Center for Toxicological Research, Jefferson, AR, is recognized for his mass spectral measurements of Tp*NiCysEt and Tp^{PhMe}NiCysEt. The National Science Foundation (DUE 9750591) is recognized for funding of a magnetic susceptibility balance used in this work. Funding for this research was provided by the University of Central Arkansas and the Arkansas SILO Advisory Council Undergraduate Research Program.

Supporting Information Available: Additional synthetic and chromatographic details, stoichiometric measurements for Tp*NiCysEt + O_2, mass spectral data, listings of fractional atomic coordinates, anisotropic thermal parameters, complete interatomic distances, and bond angles. This material is available free of charge via the Internet at http://pubs.acs.org.

IC990059A

(33) *Survey of Progress in Chemistry;* Scott, A. F., Ed.; Academic Press: New York, 1973; Vol. 6, pp 27 and 31.

(34) Mirza, S. A.; Pressler, M. A.; Kumar, M.; Day, R. O.; Maroney, M. J. *Inorg. Chem.* **1993**, *32*, 977.